Supporting Information for Bare and Ligand Protected Planar Hexacoordinate Silicon in $SiSb_3M_3^+$ (M = Ca, Sr, Ba) clusters

Chen Chen,[a] Meng-hui Wang,[a] Lin-Yan Feng,[b] Lian-Qing Zhao,[b] Jin-Chang Guo,*[b] Hua-Jin Zhai,*[b] Zhong-hua Cui,*[a] Sudip Pan,*[c] and Gabriel Merino.*[d]

[a]*Institute of Atomic and Molecular Physics, Key Laboratory of Physics and Technology for Advanced Batteries (Ministry of Education), Jilin University, Changchun 130021, China*

E-mail: zcui@jlu.edu.cn

[b]*Nanocluster Laboratory, Institute of Molecular Science, Shanxi University, Taiyuan 030006, China*

E-mail: guojc@sxu.edu.cn; hj.zhai@sxu.edu.cn

[c]*Fachbereich Chemie, Philipps-Universität Marburg, Hans-Meerwein-Strasse 4, 35032 Marburg, Germany*

E-mail: pans@chemie.uni-marburg.de

[d]*Departamento de Física Aplicada, Centro de Investigación y de Estudios Avanzados, Unidad Mérida, km 6 Antigua carretera a Progreso, Apdo. Postal 73, Cordemex 97310, Mérida, Yuc., México.*

E-mail: gmerino@cinvestav.mx

Computational methods

The potential energy surface (PES) exploration of $SiE_3M_3^+$ (E = N, P, As, Sb; M = Ca, Sr, Ba) clusters was performed using the particle swarm optimization (PSO) algorithm as implemented in the CALYPSO code.[1,2] The random structures generated

were initially optimized at the PBE0/def2-SVP level.[3,4] Further optimizations of the low-lying energy isomers were done at the PBE0/def2-TZVP level,[3,4] followed by the harmonic vibrational frequency calculations. For ligand bound $SiSb_3M_3^+$ complexes, the calculations were performed at the PBE0-D3(BJ)/def2-TZVP level. The energies for low-lying isomers were further refined using the single-point energy calculations at the CCSD(T)[5]/def2-TZVP//PBE0/def2-TZVP level. The total energies were corrected by the zero-point energies (ZPE) of PBE0. The BOMD (Born-Oppenheimer molecular dynamics) simulations[6] at room temperature (298 K) were computed at the PBE0/def2-SVP level. The electronic and bonding properties of the global minimum (GM) phSi clusters were performed by the natural bond orbital (NBO)[7,8] and adaptive natural density partitioning (AdNDP)[9] analyses. The iso-chemical shielding surface (ICSS)[10] calculations and the quantum theory of atoms in molecules (QTAIM)[11] analysis were carried out using the Multiwfn program. All the above calculations were performed using the GAUSSIAN 09 package.[12] The IQA[11] and EDA[13-15] analyses were carried out using the ADF package.[16]

References

[1] J. Lv, Y. C. Wang, L. Zhu, Y. M. Ma, *J. Chem. Phys.* **2012**, *137*, 084104.

[2] Y. C. Wang, J. Lv, L. Zhu, Y. M. Ma, *Comput. Phys. Commun.* **2012**, *183*, 2063-2070.

[3] F. Weigend, R. Ahlrichs, *Phys. Chem. Chem. Phys.* **2005**, *7*, 3297-3305.

[4] F. Weigend, *Phys. Chem. Chem. Phys.* **2006**, *8*, 1057-1065.

[5] R. J. Bartlett, M. Musiał, *Rev. Mod. Phys.* **2007**, *79*, 291-352.

[6] J. M. Millam, V. Bakken, W. Chen, W. L. Hase, H. B. Schlegel, *J. Chem. Phys.* **1999**, *111*, 3800-3805.

[7] A. E. Reed, R. B. Weinstock, F. Weinhold, *J. Chem. Phys.* **1985**, *83*, 735-746.

[8] A. E. Reed, F. Weinhold, *J. Chem. Phys.* **1983**, *78*, 4066-4073.

[9] D. Y. Zubarev, A. I. Boldyrev, *Phys. Chem. Chem. Phys.* **2008**, *10*, 5207-5217.

[10] Z. F. Chen, C. S. Wannere, C. Corminboeuf, R. Puchta, P. V. R. Schleyer, *Chem.*

Rev. **2005**, *105*, 3842-3888.

[11] F. Corts-Guzman, R. F. W. Bader, *Coord. Chem. Rev.* **2005**, *249*, 633-662.

[12] M. J. Frisch, G. W. Trucks, H. B. Schlegel, G. E. Scuseria, M. A. Robb, J. R. Cheeseman, G. Scalmani, V. Barone, B. Mennucci, G. A. Petersson, H. Nakatsuji, M. Caricato, X. Li, H. P. Hratchian, A. F. Izmaylov, J. Bloino, G. Zheng, J. L. Sonnenberg, M. Hada, M. Ehara, K. Toyota, R. Fukuda, J. Hasegawa, M. Ishida, T. Nakajima, Y. Honda, O. Kitao, H. Nakai, T. Vreven, J. A. Montgomery, J. E. Peralta, F. Ogliaro, M. Bearpark, J. J. Heyd, E. Brothers, K. N. Kudin, V. N. Staroverov, R. Kobayashi, J. Normand, K. Raghavachari, A. Rendell, J. C. Burant, S. S. Iyengar, J. Tomasi, M. Cossi, N. Rega, N. J. Millam, M. Klene, J. E. Knox, J. B. Cross, V. Bakken, C. Adamo, J. Jaramillo, R. Gomperts, R. E. Stratmann, O. Yazyev, A. J. Austin, R. Cammi, C. Pomelli, J. W. Ochterski, R. L. Martin, K. Morokuma, V. G. Zakrzewski, G. A. Voth, P. Salvador, J. J. Dannenberg, S. Dapprich, A. D. Daniels, O. Farkas, J. B. Foresman, J. V. Ortiz, J. Cioslowski, D. J. Fox, *Gaussian 09 Revision D.01*, Gaussian, Inc., Wallingford CT, 2009.

[13] T. Ziegler, A. Rauk, *Theoret. Chim. Acta.* **1977**, *46*, 1-10.

[14] L. L. Zhao, M. vonHopffgarten, D. M. Andrada, G. Frenking, *WIREs Comput. Mol. Sci.* **2018**, *8*, e1345.

[15] L. L. Zhao, M. Hermann, W. E. Schwarz, G. Frenking, *Nat. Rev. Chem.* **2019**, *3*, 48-63.

[16] G. t. Velde, F. M. Bickelhaupt, E. J. Baerends, C. F. Guerra, S. J. A. V. Gisbergen, J. G. Snijders, T. Ziegler, *J. Comput. Chem.* **2001**, *22*, 931-967.

Aromaticity analyses

The aromaticity character of the title phSi clusters is uncovered by the iso-chemical shielding surface (ICSS), that is, the isosurface of the nucleus-independent chemical shifts (NICSs). The ICSS calculations present an exceedingly intuitive picture on aromaticity. The $ICSS_{zz}(1)$ (a z-direction component of $ICSS_{zz}$ at 1.0 Å above the molecular plane) is displayed in Figure S9b and Figure S10. The phSi $SiE_3Ca_3^+$ cluster clearly displays a weak aromaticity for the whole plane, featuring a sharp change from Si-E bonds to the neighboring region, indicating −20.0 ppm at Si-Sb region to +4.6 ppm (Si-Ca) and −5.3 ppm (Sb-Si-C triangle) as given Figure S9c. The canonical molecular orbital (MO) dissection into π orbitals of $NICS_{zz}$ grid is given in Figure S9d, where $NICS_{zz}$ (π electrons) is clearly smaller as compared to total $NICS_{zz}$. Additionally, the strong electron localization within Si-E multiple bonds is also found in the electron localization function (ELF) picture in Figure S9a.

Table S1. Calculated lowest vibrational frequencies (ν_{min}, cm^{-1}) and natural atomic charges (q, in |e|) for $SiE_3M_3^+$ (E = S−Po; M = Li–Cs) clusters at the PBE0-D3/def2-TZVPP level.

System	Symmetry	ν_{min}	q (Si)	q (E)	q (M)
$SiS_3Li_3^+$	D_{3h}	51	+0.88	–0.83	+0.87
$SiS_3Na_3^+$	D_{3h}	42	+0.97	–0.91	+0.92
$SiS_3K_3^+$	D_{3h}	37	+1.03	–0.94	+0.93
$SiS_3Rb_3^+$	D_{3h}	29	+1.03	–0.96	+0.95
$SiS_3Cs_3^+$	D_{3h}	19	+1.03	–0.96	+0.95
$SiSe_3Li_3^+$	C_{3v}	30	+0.58	–0.69	+0.83
$SiSe_3Na_3^+$	D_{3h}	28	+0.67	–0.80	+0.91
$SiSe_3K_3^+$	D_{3h}	26	+0.70	–0.82	+0.92
$SiSe_3Rb_3^+$	D_{3h}	20	+0.73	–0.84	+0.93
$SiSe_3Cs_3^+$	D_{3h}	16	+0.76	–0.86	+0.94
$SiTe_3Li_3^+$	C_{3v}	70	+0.10	–0.44	+0.74
$SiTe_3Na_3^+$	D_{3h}	10	+0.22	–0.61	+0.87
$SiTe_3K_3^+$	D_{3h}	18	+0.28	–0.64	+0.88
$SiTe_3Rb_3^+$	D_{3h}	13	+0.31	–0.67	+0.90
$SiTe_3Cs_3^+$	D_{3h}	11	+0.28	–0.68	+0.92
$SiPo_3Li_3^+$	C_{3v}	63	+0.01	–0.37	+0.70
$SiPo_3Na_3^+$	C_{3v}	25	+0.07	–0.54	+0.85
$SiPo_3K_3^+$	D_{3h}	12	+0.16	–0.60	+0.88
$SiPo_3Rb_3^+$	D_{3h}	9	+0.19	–0.63	+0.90
$SiPo_3Cs_3^+$	D_{3h}	7	+0.19	–0.65	+0.92

Table S2. Bond properties (*r*, distances in Å) and NPA charges (q, |e|) of the phSi $SiE_3Sr_3^+$ (E = N, P, As, Sb) clusters at the PBE0/def2-TZVP level.

$SiE_3Sr_3^+$	r_{Si-E}	r_{Si-Sr}	r_{E-Sr}	q_{Si}	q_E	q_{Sr}
E = N	1.675	2.710	2.369	1.62	-1.96	1.75
E = P	2.184	3.121	2.774	0.31	-1.45	1.68
E = As	2.303	3.200	2.859	0.14	-1.37	1.66
E = Sb	2.536	3.366	3.037	-0.31	-1.20	1.63

Table S3. Bond properties (*r*, distances in Å) and NPA charges (q, |e|) of phSi $SiE_3Ba_3^+$ (E = N, P, As, Sb) clusters obtained at the PBE0/def2-TZVP level.

$SiE_3Ba_3^+$	r_{Si-E}	r_{Si-Ba}	r_{E-Ba}	q_{Si}	q_E	q_{Ba}
E = N	1.678	2.859	2.489	1.65	-1.97	1.76
E = P	2.185	3.300	2.907	0.34	-1.45	1.67
E = As	2.304	3.387	2.996	0.17	-1.39	1.66
E = Sb	2.533	3.566	3.178	-0.28	-1.20	1.63

Table S4. The bond order analysis of $SiE_3Sr_3^+$ (E = N, P, As, Sb) clusters computed at the PBE0/def2-TZVP level.

		Si-E	Si-Sr	E-Sr
Wiberg bond order	E = N	1.13	0.02	0.21
	E = P	1.33	0.03	0.28
	E = As	1.32	0.03	0.28
	E = Sb	1.29	0.04	0.30
Mayer bond order	E = N	1.31	0.14	0.57
	E = P	1.16	0.13	0.69
	E = As	1.16	0.14	0.67
	E = Sb	1.06	0.14	0.71
Wiberg bond order analysis in Lowdin orthogonalized basis	E = N	1.83	0.50	0.84
	E = P	1.53	0.51	1.05
	E = As	1.46	0.52	1.11
	E = Sb	1.35	0.45	1.14

Table S5. The bond order analysis of $SiE_3Ba_3^+$ (E = N, P, As, Sb) clusters computed at the PBE0/def2-TZVP level.

		Si-E	Si-Ba	E-Ba
Wiberg bond order	E = N	1.12	0.02	0.21
	E = P	1.32	0.03	0.27
	E = As	1.31	0.03	0.28
	E = Sb	1.28	0.04	0.31
Mayer bond order	E = N	1.31	0.17	0.54
	E = P	1.20	0.10	0.61
	E = As	1.19	0.10	0.62
	E = Sb	1.14	0.10	0.61
Wiberg bond order analysis in Lowdin orthogonalized basis	E = N	1.85	0.52	0.84
	E = P	1.58	0.48	1.05
	E = As	1.51	0.49	1.12
	E = Sb	1.39	0.42	1.15

Table S6. The EDA results of SiN_3Ca_3 cluster using Ca and SiN_3Ca_2 in different charge and electronic states as interacting fragments at the PBE0/TZ2P-ZORA//PBE0/def2-TZVP level. All energy values in kcal/mol.

Energy Term	Ca^+ (D, $4s^1$) + SiN_3Ca_2 (D)	Ca^{2+} (S, $4s^0$) + $SiN_3Ca_2^-$ (S)	Ca (T, $4s^14d^1$) + $SiN_3Ca_2^+$ (T)
ΔE_{int}	-192.9	-428.5	-210.7
ΔE_{Pauli}	139.8	112.3	96.0
ΔE_{elstat}	-162.0	-356.6	-125.6
ΔE_{orb}	-170.7	-184.2	-181.1

Table S7. The EDA results of SiP_3Ca_3 cluster using Ca and SiP_3Ca_2 in different charge and electronic states as interacting fragments at the PBE0/TZ2P-ZORA//PBE0/def2-TZVP level. All energy values in kcal/mol.

Energy Term	Ca^+ (D, $4s^1$) + SiP_3Ca_2 (D)	Ca^{2+} (S, $4s^0$) + $SiP_3Ca_2^-$ (S)	Ca (T, $4s^14d^1$) + $SiP_3Ca_2^+$ (T)
ΔE_{int}	-153.0	-371.3	-198.8
ΔE_{Pauli}	115.2	86.2	123.1
ΔE_{elstat}	-116.4	-285.4	-90.3
ΔE_{orb}	-151.8	-172.2	-231.6

Table S8. The EDA results of $SiAs_3Ca_3$ cluster using Ca and $SiAs_3Ca_2$ in different charge and electronic states as interacting fragments at the PBE0/TZ2P-ZORA//PBE0/def2-TZVP level. All energy values in kcal/mol.

Energy Term	Ca^+ (D, $4s^1$) + $SiAs_3Ca_2$ (D)	Ca^{2+} (S, $4s^0$) + $SiAs_3Ca_2^-$ (S)	Ca (T, $4s^14d^1$) + $SiAs_3Ca_2^+$ (T)
ΔE_{int}	-144.9	-361.6	-187.7
ΔE_{Pauli}	115.7	79.3	127.5
ΔE_{elstat}	-113.0	-266.4	-96.9
ΔE_{orb}	-147.6	-174.5	-218.3

Table S9. The EDA results of $SiSb_3Ca_3$ cluster using Ca and $SiSb_3Ca_2$ in different charge and electronic states as interacting fragments at the PBE0/TZ2P-ZORA//PBE0/def2-TZVP level. All energy values in kcal/mol.

Energy Term	Ca^+ (D, $4s^1$) + $SiSb_3Ca_2$ (D)	Ca^{2+} (S, $4s^0$) + $SiSb_3Ca_2^-$ (S)	Ca (T, $4s^14d^1$) + $SiSb_3Ca_2^+$ (T)
ΔE_{int}	-129.9	-342.9	-169.5
ΔE_{Pauli}	110.9	69.6	130.3
ΔE_{elstat}	-100.9	-237.0	-102.0
ΔE_{orb}	-140.0	-175.6	-197.7

Table S10. Energy components of interacting quantum atoms (IQA) analysis in kcal/mol for the D_{3h}-symmetric phSi $SiE_3Ca_3^+$ (E = N, P, As, Sb) systems. The inter-atomic interaction energy (V_{Total}) can be evaluated and decomposed into electrostatic (ionic, V_{Ionic}) and exchange (covalent, $V_{Coval.}$) contributions.

$SiE_3Ca_3^+$	$SiN_3Ca_3^+$	$SiP_3Ca_3^+$	$SiAs_3Ca_3^+$	$SiSb_3Ca_3^+$
V_{Total} (Si-E)	-1232.1	-450.7	-247.6	-118.9
V_{Ionic} (Si-E)	-1117.6	-303.5	-95.1	25.2
$V_{Coval.}$ (Si-E)	-114.5	-147.1	-152.5	-144.1
V_{Total} (Si-Ca)	509.8	194.7	80.7	**-40.2**
V_{Ionic} (Si-Ca)	515.2	202.9	90.6	**-28.6**
$V_{Coval.}$ (Si-Ca)	-5.5	-8.2	-10.0	**-11.6**
V_{Total} (E-Ca)	-476.4	-303.9	-252.7	-185.4
V_{Ionic} (E-Ca)	-413.1	-249.8	-201.6	-136.1
$V_{Coval.}$ (E-Ca)	-63.3	-54.1	-51.1	-49.4

Table S11. Energy components of interacting quantum atoms (IQA) analysis in kcal/mol for the D_{3h}-symmetric phSi $SiE_3Sr_3^+$ (E = N, P, As, Sb) systems. The inter-atomic interaction energy (V_{Total}) can be evaluated and decomposed into electrostatic (ionic, V_{Ionic}) and exchange (covalent, $V_{Coval.}$) contributions.

$SiE_3Sr_3^+$	$SiN_3Sr_3^+$	$SiP_3Sr_3^+$	$SiAs_3Sr_3^+$	$SiSb_3Sr_3^+$
V_{Total} (Si-E)	-1230.6	-447.3	-246.7	-120.7
V_{Ionic} (Si-E)	-1116.9	-300.6	-94.8	23.4
$V_{Coval.}$ (Si-E)	-113.7	-146.8	-151.9	-144.1
V_{Total} (Si-Sr)	505.4	187.9	80.1	**-35.4**
V_{Ionic} (Si-Sr)	510.1	195.5	89.3	**-25.1**
$V_{Coval.}$ (Si-Sr)	-4.6	-7.6	-9.2	**-10.3**
V_{Total} (E-Sr)	-477.0	-296.6	-246.4	-182.3
V_{Ionic} (E-Sr)	-413.5	-242.3	-194.9	-132.8
$V_{Coval.}$ (E-Sr)	-63.5	-54.4	-51.6	-49.5

Table S12. Energy components of interacting quantum atoms (IQA) analysis in kcal/mol for the D_{3h}-symmetric phSi $SiE_3Ba_3^+$ (E = N, P, As, Sb) systems. The inter-atomic interaction energy (V_{Total}) can be evaluated and decomposed into electrostatic (ionic, V_{Ionic}) and exchange (covalent, $V_{Coval.}$) contributions.

$SiE_3Ba_3^+$	$SiN_3Ba_3^+$	$SiP_3Ba_3^+$	$SiAs_3Ba_3^+$	$SiSb_3Ba_3^+$
V_{Total} (Si-E)	-1204.1	-433.2	-240.2	-123.0
V_{Ionic} (Si-E)	-1093.1	-289.4	-90.7	18.4
$V_{Coval.}$ (Si-E)	-111.1	-143.8	-149.5	-141.4
V_{Total} (Si-Ba)	472.4	168.6	73.0	**-27.4**
V_{Ionic} (Si-Ba)	477.5	176.9	82.7	**-16.5**
$V_{Coval.}$ (Si-Ba)	-5.2	-8.4	-9.7	**-10.9**
V_{Total} (E-Ba)	-444.8	-261.2	-219.0	-160.2
V_{Ionic} (E-Ba)	-372.4	-199.0	-160.4	-104.1
$V_{Coval.}$ (E-Ba)	-72.4	-62.2	-58.6	-56.1

Table S13. IQA analysis in kcal/mol of $SiSb_3M_3(NHC)_6^+$ and $SiSb_3M_3(Bz)_6^+$ complexes (M = Ca, Sr, Ba) computed at the PBE0/TZ2P-ZORA level, where inter-atomic interaction energy (V_{Total}) can be evaluated and decomposed into electrostatic (ionic, V_{Ionic}) and exchange (covalent, $V_{Coval.}$) contributions.

	$SiSb_3Ca_3(NHC)_6^+$	$SiSb_3Sr_3(NHC)_6^+$	$SiSb_3Ba_3(NHC)_6^+$	$SiSb_3Ca_3(NHC)_6^+$	$SiSb_3Sr_3(NHC)_6^+$	$SiSb_3Ba_3(NHC)_6^+$
V_{Total} (Si-Sb)	-125.8	-125.4	-125.2	-123.1	-124.0	-128.2
V_{Ionic} (Si-Sb)	19.4	17.7	19.3	24.6	22.1	13.0
$V_{Coval.}$ (Si-Sb)	-145.2	-143.1	-144.6	-147.7	-146.1	-141.2
V_{Total} (Si-Ca)	**-24.5**	**-22.2**	**-23.7**	**-32.4**	**-27.8**	**-20.0**
V_{Ionic} (Si-Ca)	**-17.8**	**-15.7**	**-16.6**	**-25.8**	**-21.1**	**-13.8**
$V_{Coval.}$ (Si-Ca)	**-6.7**	**-6.5**	**-7.1**	**-6.6**	**-6.7**	**-6.2**
V_{Total} (Sb-Ca)	-204.6	-194.6	-160.5	-185.1	-181.0	-183.2
V_{Ionic} (Sb-Ca)	-172.4	-159.4	-117.8	-152.0	-145.0	-144.7
$V_{Coval.}$ (Sb-Ca)	-32.2	-35.3	-42.7	-33.1	-36.0	-38.5

Table S13. Cartesian coordinates of phSi $SiE_3M_3^+$ (E = N, P, As, Sb, M = Ca, Sr, Ba) clusters at the PBE0/def2-TZVP level.

$SiN_3Ca_3^+$
ν_{min} = 67.1 cm^{-1}
HF = -2485.719814 a.u.

Si	0.000000000000	0.000000000000	0.000000000000
N	-1.669773000000	0.000000000000	0.000000000000
N	0.834886000000	1.446066000000	0.000000000000
N	0.834886000000	-1.446066000000	0.000000000000
Ca	-1.277232000000	2.212231000000	0.000000000000
Ca	2.554464000000	0.000000000000	0.000000000000
Ca	-1.277232000000	-2.212231000000	0.000000000000

$SiP_3Ca_3^+$
ν_{min} = 47.5 cm^{-1}
HF = -3345.342821 a.u.

Si	0.000000000000	0.000000000000	0.000000000000
P	1.089857000000	-1.887688000000	0.000000000000
P	1.089857000000	1.887688000000	0.000000000000
P	-2.179714000000	0.000000000000	0.000000000000
Ca	2.935032000000	0.000000000000	0.000000000000
Ca	-1.467516000000	2.541812000000	0.000000000000
Ca	-1.467516000000	-2.541812000000	0.000000000000

$SiAs_3Ca_3^+$
ν_{min} = 34.5 cm^{-1}
HF = -9028.496686 a.u.

Si	0.000000000000	0.000000000000	0.000000000000
As	1.150288000000	-1.992357000000	0.000000000000
As	1.150288000000	1.992357000000	0.000000000000
As	-2.300575000000	0.000000000000	0.000000000000
Ca	3.003801000000	0.000000000000	0.000000000000
Ca	-1.501901000000	2.601368000000	0.000000000000
Ca	-1.501901000000	-2.601368000000	0.000000000000

$SiSb_3Ca_3^+$
ν_{min} = 15.6 cm^{-1}
HF = -3042.453846 a.u.

Si	0.000000000000	0.000000000000	0.000000000000
Sb	1.268800000000	-2.197626000000	0.000000000000
Sb	1.268800000000	2.197626000000	0.000000000000
Sb	-2.537600000000	0.000000000000	0.000000000000
Ca	3.154735000000	0.000000000000	0.000000000000

Ca	-1.577368000000	2.732081000000	0.000000000000
Ca	-1.577368000000	-2.732081000000	0.000000000000

$SiN_3Sr_3^+$
ν_{min} = 67.3 cm^{-1}
HF = -545.615826 a.u.

Si	0.000000000000	0.000000000000	0.000000000000
N	0.000000000000	1.675250000000	0.000000000000
N	1.450809000000	-0.837625000000	0.000000000000
N	-1.450809000000	-0.837625000000	0.000000000000
Sr	2.347148000000	1.355127000000	0.000000000000
Sr	0.000000000000	-2.710254000000	0.000000000000
Sr	-2.347148000000	1.355127000000	0.000000000000

$SiP_3Sr_3^+$
ν_{min} = 40.4 cm^{-1}
HF = -1405.256070 a.u.

Si	0.000000000000	0.000000000000	0.000000000000
P	0.000000000000	2.184008000000	0.000000000000
P	-1.891406000000	-1.092004000000	0.000000000000
P	1.891406000000	-1.092004000000	0.000000000000
Sr	-2.703094000000	1.560632000000	0.000000000000
Sr	0.000000000000	-3.121264000000	0.000000000000
Sr	2.703094000000	1.560632000000	0.000000000000

$SiAs_3Sr_3^+$
ν_{min} = 28.7 cm^{-1}
HF = -7088.409963 a.u.

Si	0.000000000000	0.000000000000	0.000000000000
As	-1.994637000000	-1.151604000000	0.000000000000
As	0.000000000000	2.303208000000	0.000000000000
As	1.994637000000	-1.151604000000	0.000000000000
Sr	-2.770856000000	1.599755000000	0.000000000000
Sr	2.770856000000	1.599755000000	0.000000000000
Sr	0.000000000000	-3.199509000000	0.000000000000

$SiSb_3Sr_3^+$
ν_{min} = 16.7 cm^{-1}
HF = -1102.368836 a.u.

Si	0.000000000000	0.000000000000	0.000000000000
Sb	0.000000000000	2.536412000000	0.000000000000
Sb	2.196597000000	-1.268206000000	0.000000000000
Sb	-2.196597000000	-1.268206000000	0.000000000000
Sr	2.914659000000	1.682779000000	0.000000000000

Sr	0.000000000000	-3.365559000000	0.000000000000
Sr	-2.914659000000	1.682779000000	0.000000000000

$SiN_3Ba_3^+$
ν_{min} = 16.7 cm^{-1}
HF = -1102.368836 a.u.

Si	0.000000000000	0.000000000000	0.000000000000
N	1.677044000000	0.000000000000	0.000000000000
N	-0.838522000000	-1.452362000000	0.000000000000
N	-0.838522000000	1.452362000000	0.000000000000
Ba	1.429840000000	-2.476555000000	0.000000000000
Ba	-2.859679000000	0.000000000000	0.000000000000
Ba	1.429840000000	2.476555000000	0.000000000000

$SiP_3Ba_3^+$
ν_{min} = 36.2 cm^{-1}
HF = -1389.631282 a.u.

Si	0.000000000000	0.000000000000	0.000000000000
P	0.000000000000	2.184787000000	0.000000000000
P	-1.892081000000	-1.092394000000	0.000000000000
P	1.892081000000	-1.092394000000	0.000000000000
Ba	-2.857834000000	1.649971000000	0.000000000000
Ba	0.000000000000	-3.299942000000	0.000000000000
Ba	2.857834000000	1.649971000000	0.000000000000

$SiAs_3Ba_3^+$
ν_{min} = 25.1 cm^{-1}
HF = -7072.786148 a.u.

Si	0.000000000000	0.000000000000	0.000000000000
As	0.000000000000	2.303744000000	0.000000000000
As	1.995101000000	-1.151872000000	0.000000000000
As	-1.995101000000	-1.151872000000	0.000000000000
Ba	2.933596000000	1.693712000000	0.000000000000
Ba	0.000000000000	-3.387425000000	0.000000000000
Ba	-2.933596000000	1.693712000000	0.000000000000

$SiSb_3Ba_3^+$
ν_{min} = 16.5 cm^{-1}
HF = -1086.745890 a.u.

Si	0.000000000000	0.000000000000	0.000000000000
Sb	2.193372000000	-1.266344000000	0.000000000000
Sb	0.000000000000	2.532688000000	0.000000000000
Sb	-2.193372000000	-1.266344000000	0.000000000000
Ba	3.088241000000	1.782997000000	0.000000000000

Ba	-3.088241000000	1.782997000000	0.000000000000
Ba	0.000000000000	-3.565994000000	0.000000000000

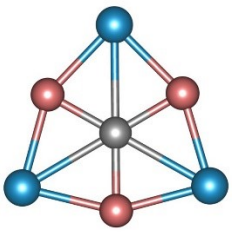

	$SiN_3M_3^+$	$SiP_3M_3^+$	$SiAs_3M_3^+$	$SiSb_3M_3^+$	$SiBi_3M_3^+$
M = Be	307.0*i*	208.3*i*	205.4*i*	210.1*i*	225.2*i*
M = Mg	62.5*i*	94.2*i*	100.5*i*	116.1*i*	128.2*i*
M = Ca	67.1	47.5	34.6	15.6	9.2*i*
M = Sr	64.1	41.8	28.5	16.8	9.6
M = Ba	65.6	36.0	25.1	16.9	11.5

Figure S1. The lowest vibrational frequencies (ν_{min}, cm^{-1}) of $SiE_3M_3^+$ (E = N, P, As, Sb, Bi; M = Be, Mg, Ca, Sr, Ba) clusters at the PBE0/def2-TZVP level.

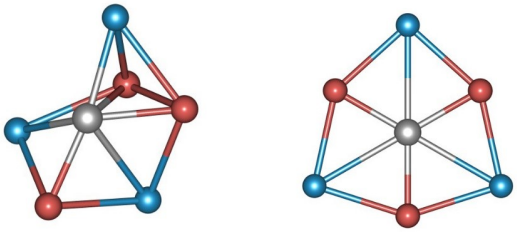

Figure S2. The relative energies in kcal/mol of the lowest-energy isomer and the phSi structure of $SiBi_3M_3^+$ (M = Sr, Ba) clusters at the CCSD(T)/def2-TZVP//PBE0/def2-TZVP level. Total energies are corrected by the zero-point energies (ZPEs) and the Ba-based cases given in parentheses.

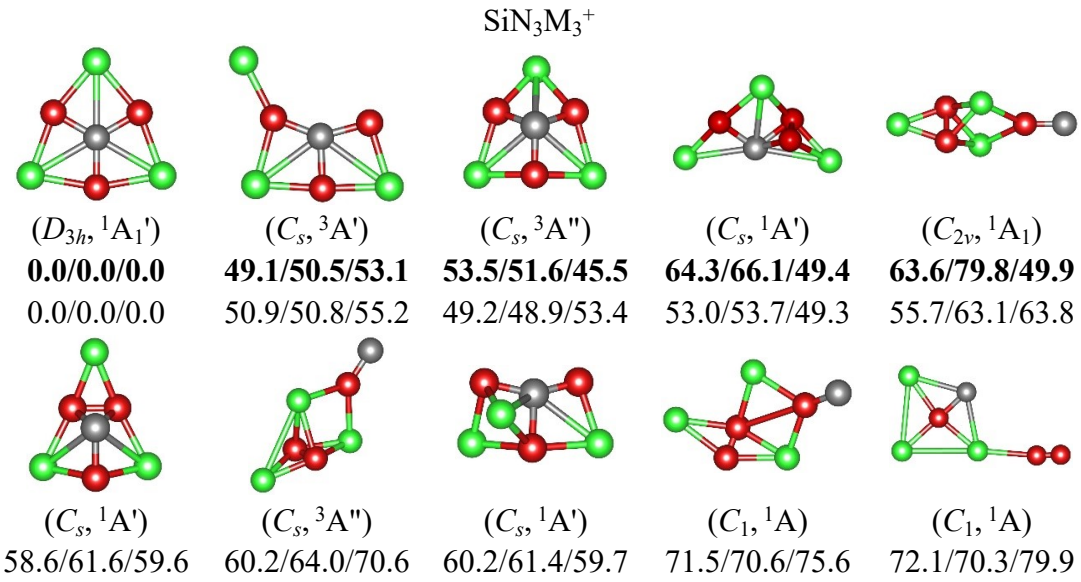

Figure S3. Structures and relative energies in kcal/mol of the low-lying isomers of $SiN_3M_3^+$ (M = Ca, Sr, Ba) clusters at the single-point CCSD(T)/def2-TZVP//PBE0/def2-TZVP (in bold) and PBE0/def2-TZVP levels. All energies are corrected by ZPEs at PBE0/def2-TZVP, and the values from left to right refer to Ca, Sr, and Ba in sequence. The point group symmetries and electronic states are given in parentheses.

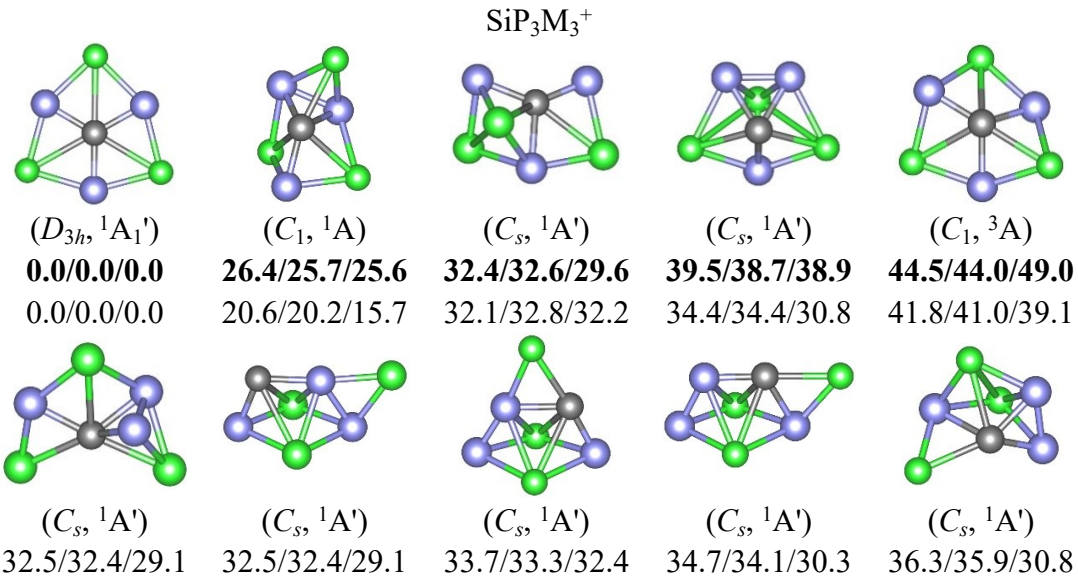

Figure S4. Structures and relative energies in kcal/mol of the low-lying isomers of $SiP_3M_3^+$ (M = Ca, Sr, Ba) clusters at the single-point CCSD(T)/def2-TZVP//PBE0/def2-TZVP (in bold) and PBE0/def2-TZVP levels. All energies are corrected by ZPEs at PBE0/def2-TZVP, and the values from left to right refer to Ca, Sr, and Ba in sequence. The point group symmetries and electronic states are given in parentheses.

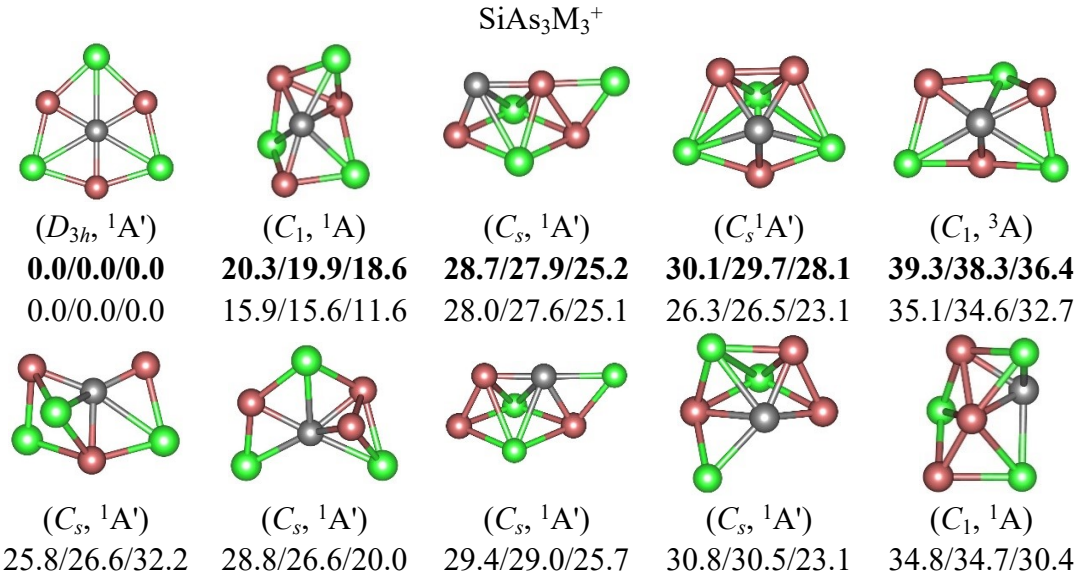

Figure S5. Structures and relative energies in kcal/mol of the low-lying energy isomers of $SiAs_3M_3^+$ (M = Ca, Sr, Ba) clusters at the single-point CCSD(T)/def2-TZVP//PBE0/def2-TZVP (in bold) and PBE0/def2-TZVP levels. All energies are corrected ZPEs at PBE0/def2-TZVP, and the values from left to right refer to Ca, Sr, and Ba in sequence. The point group symmetries and electronic states are given in parentheses.

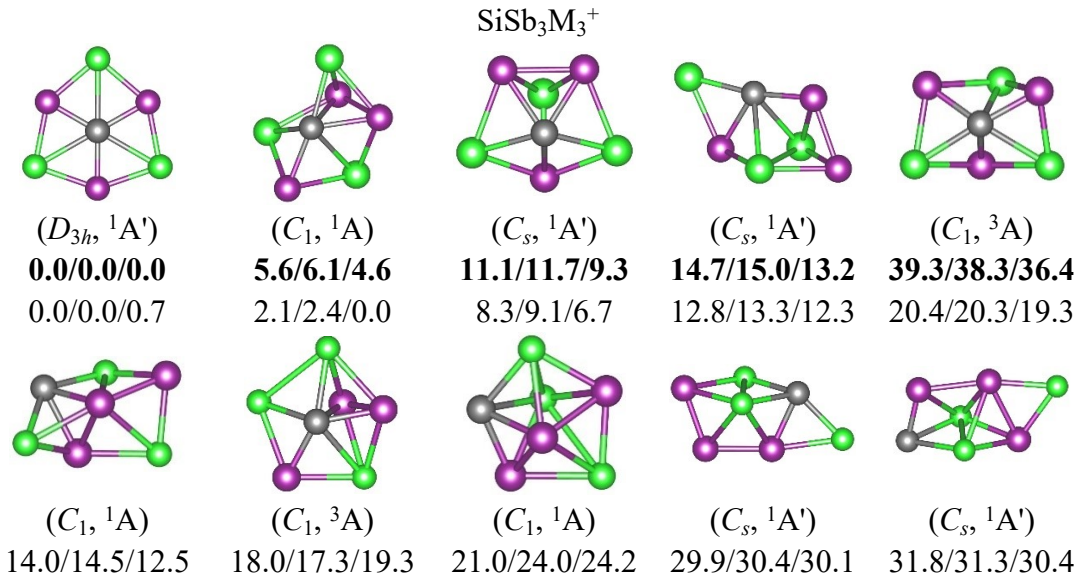

Figure S6. Structures and relative energies in kcal/mol of the low-lying energy isomers of $SiSb_3M_3^+$ (M = Ca, Sr, Ba) clusters at the single-point CCSD(T)/def2-TZVP//PBE0/def2-TZVP (in bold) and PBE0/def2-TZVP levels. All energies are corrected by ZPEs at PBE0/def2-TZVP, and the values from left to right refer to Ca, Sr, and Ba in sequence. The point group symmetries and electronic states are given in parentheses.

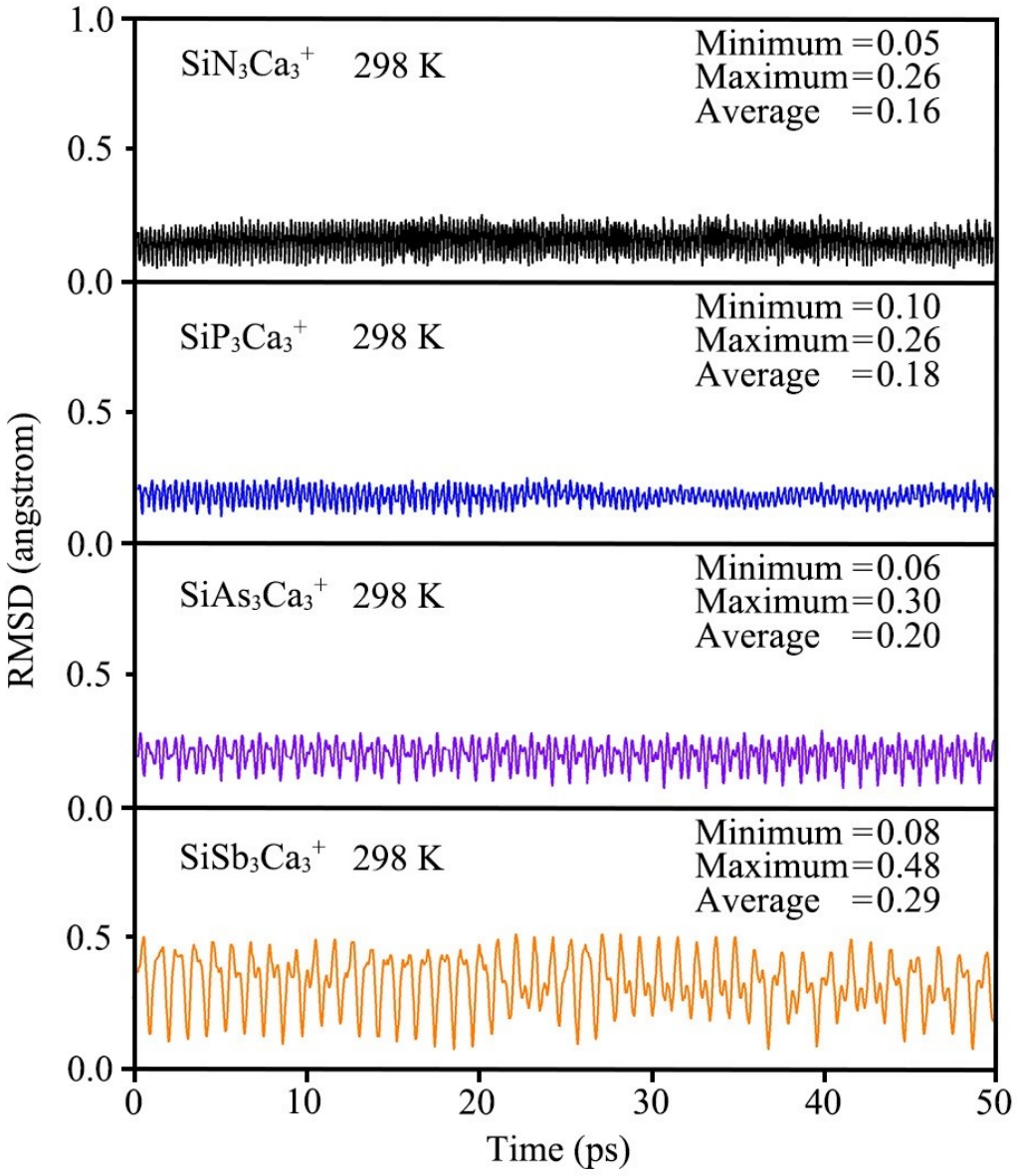

Figure S7. The plots of RMSD versus time of $SiE_3Ca_3^+$ (E = N, P, As, Sb) clusters during the BOMD simulations at 298 K at the PBE0/def2-SVP level.

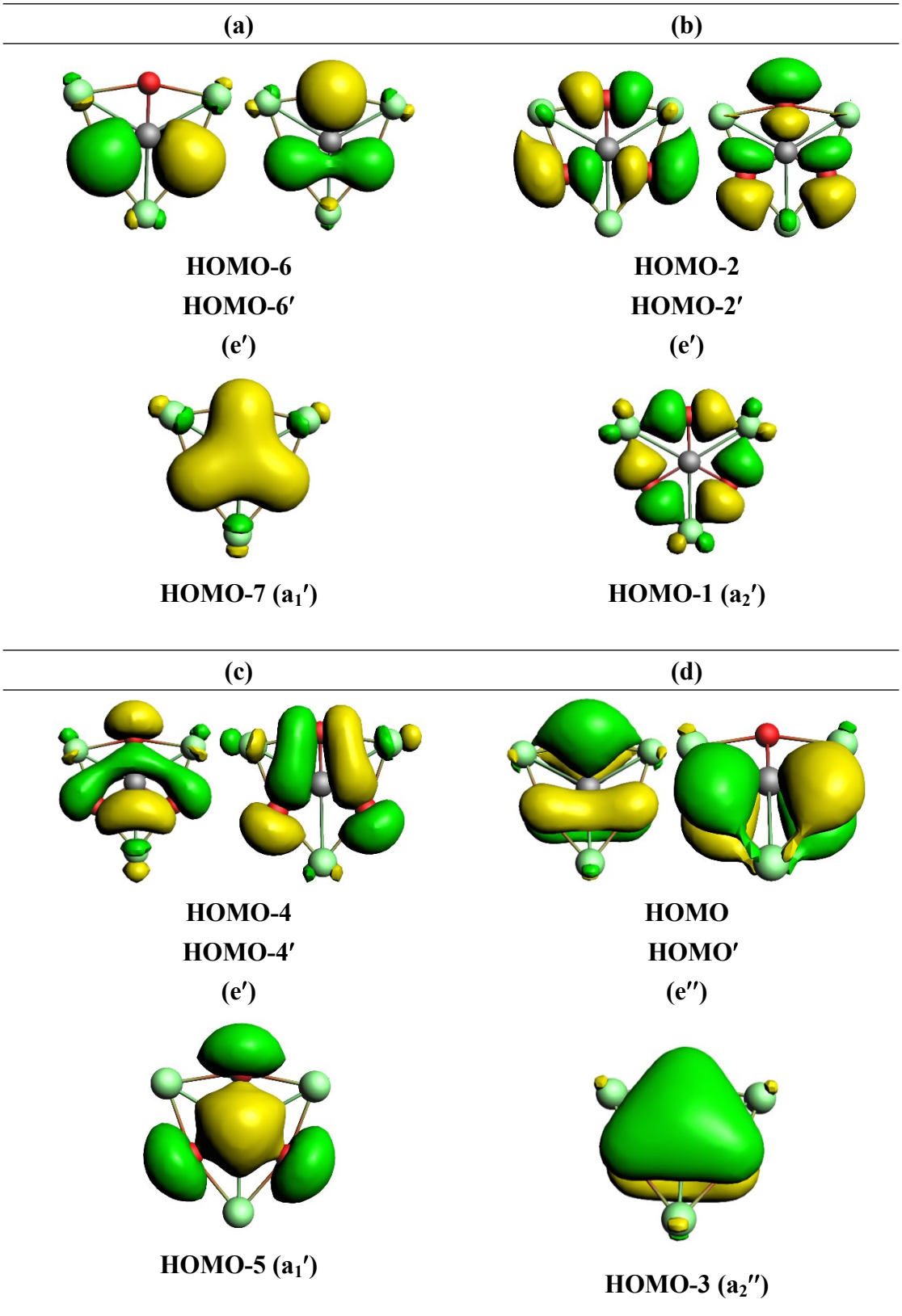

Figure S8. The pictures of the twelve occupied molecular orbitals of $SiN_3Ca_3^+$ cluster.

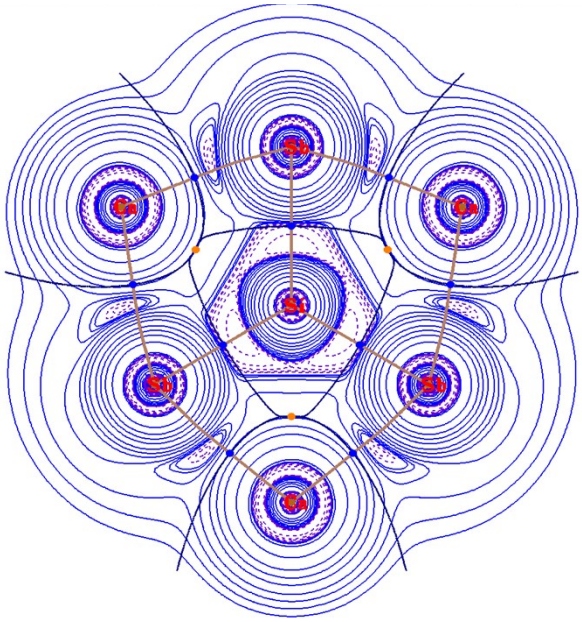

Figure S9. The plot of Laplacian of electron density along with the molecular graph of $SiSb_3Ca_3^+$ cluster. Blue dots indicate bond critical point and yellow dots indicate ring critical points. Blue solid lines and pink dotted lines show the area of $\nabla^2\rho(r) > 0$ and $\nabla^2\rho(r) < 0$, respectively.

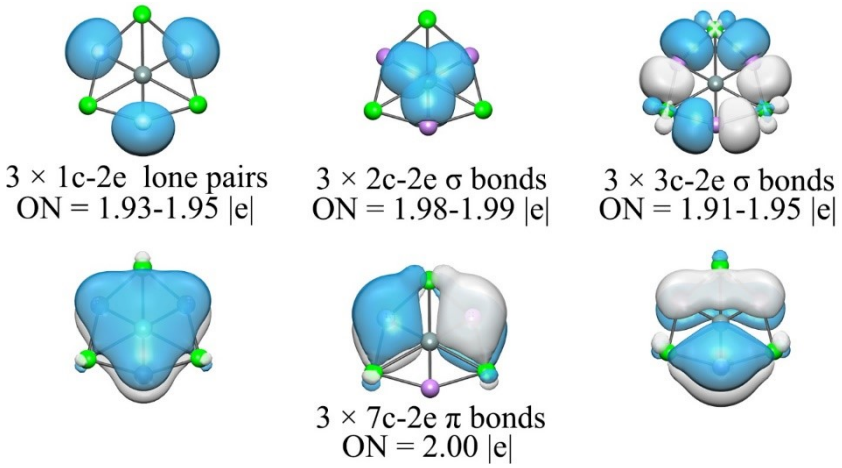

Figure S10. Comparative AdNDP schemes of $SiE_3Ca_3^+$ (E = N-Sb) cluster, and ON refers to occupation number.

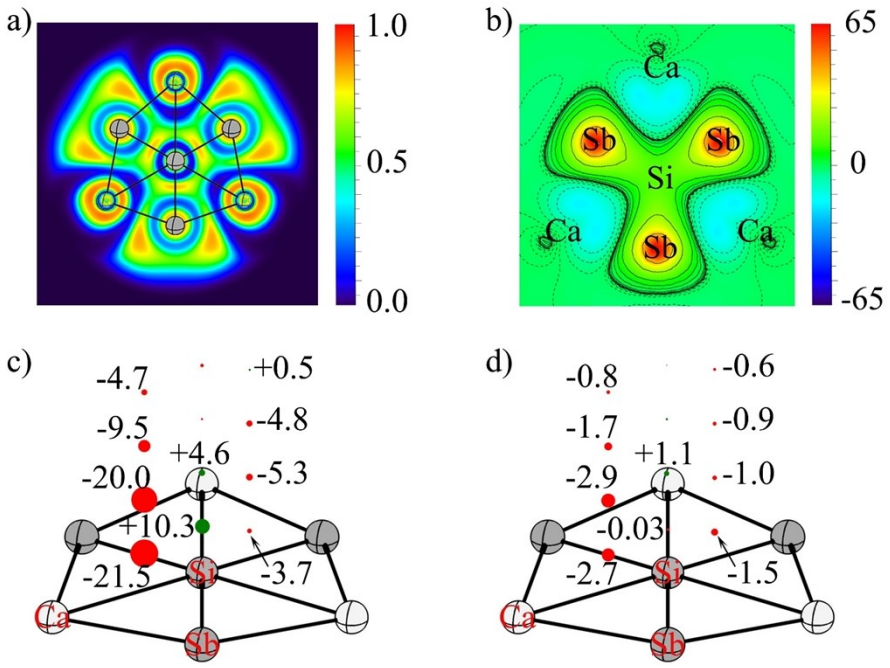

Figure S11. a) Electron localization function (ELF), b) $ICSS_{zz}$, c) $NICS_{zz}$, and d) $NICS_{zz}$ (π orbitals) for $SiSb_3Ca_3^+$ cluster. In d) the diatropic and paratropic tensors are shown in red and green, respectively. The NICS values are in ppm.